2024 IEEE/RSJ International Conference on Intelligent Robots and Systems (IROS)
October 14-18, 2024. Abu Dhabi, UAE

Climbing Gait for a Snake Robot by Adapting to a Flexible Net

Kodai Yoshida and Motoyasu Tanaka

Abstract— **This paper introduces climbing gait for the snake robot by adapting to a flexible net. A net deforms in various ways due to external forces. Therefore, we tilt snake robot's body to adapt to the deformation of the net. In addition, we can adjust the position of the head of a snake robot passing through the mesh. A snake robot can move not only vertically but also horizontally. We demonstrated the validity of the proposed method through experiments in vertical movement and movement in diagonal direction.**

I. INTRODUCTION

Net is used for a variety of purposes, such as ball catching and fall protection due to its grid-like shape. It may be torn due to wind, deterioration or flying balls. Nets are usually set at high places and the reparation by humans are highly dangerous, so it is desirable that the work is carried out by robots. In research on net movement, there is a robot that moves on a net that is used for preventing collapse by inserting claws into the mesh [1] to prevent from falling, and there is also a robot that crawls on a net in micro gravity [2]. However, in these studies, movement on deformable nets under gravitational conditions has not been realized. Nets are made up of ropes and cables, and these are similar to nets for robots. Fu et al. [3] proposed that the operation of using two grippers on a power cable made it possible for a robot to overcome obstacles and move onto an adjacent cable. In addition, the optimal control was studied that a two-brachiation robot traverse a flexible and vibrating cable [4]. However, these robots cannot move vertically.

Non wheeled snake robot can move on uneven ground [5], use obstacles [6], [7], move up and down ladders [8], move in pipes [9], [10], lift its head [11]. If a snake robot can perform net-climbing motions, the range of applications of a single robot will be expanded. The movement between different environment is realized by [12]. By applying this, after inspection of a net, a snake robot can move on the ground or uneven ground, and it can move to another net to start another inspection. In addition, the method for recovering the body shape of a snake robot when multiple joints fail is proposed by [13], and the robot can achieve the desired movement. The kinematic redundancy of the snake robot can be used to compensate for multiple joints failure, it is expected that tasks can be accomplished even when robots work for long periods of time. In [15], rope climbing is achieved using a snake robot with multiple joints and a body shape that allows the application of the principles of object grasping. However, this method can't be applied to the net climbing because there are ropes in horizontal and vertical directions unlike ropes that extend in one direction. We consider that climbing movement on a flexible net is achieved by passing the robot's body through meshes.

In this study, we propose a gait that a snake robot adapt to a flexible net in order for the robot to move in any direction. To prevent the robot from falling out the net, we take advantage of the slim body of the snake robot by passing the robot's body through the mesh. In addition, the gait is designed such that the robot's cables do not become tangled in the mesh when moving. The net will deform when the robot hangs on it, but the proposed gait allows adjustment of body shape according to this deformation. When the body through a narrow mesh, we can adjust the position of the head to enter or exit the desired mesh.

II. GAIT DESIGN AND FITTING METHOD

We use a snake robot model that has alternating pitch and yaw joints as shown in Fig. 1. There are various methods for fitting a snake robot to a continuous curve. In this study, we use the Yamada's method [16] to caluculate target joint angles, which has low computational cost and sufficient accuracy for practical use. We also design a robot's target shape using the method proposed by Takemori et al. [5].

A. Shape Fitting Using the Backbone Curve

We use the Yamada's method [16] in order to calculate each target joint angle. When a snake robot is approximated to a continuous curve, the *backbone curve*, which consider robot's posture, is used. As shown in Fig. 2, we set the *Frenet-Serret frame* $(\boldsymbol{e}_1(s), \boldsymbol{e}_2(s), \boldsymbol{e}_3(s))$ and the *backbone curve reference set* $(\boldsymbol{e}_r(s), \boldsymbol{e}_p(s), \boldsymbol{e}_y(s))$. The twist angle between the Frenet-Serret frame and the backbone reference frame around the $\boldsymbol{e}_1(s)$ shown in Fig. 2 is expressed as

$$\psi(s) = \int_0^s \tau(\hat{s})\mathrm{d}\hat{s} + \psi(0). \tag{1}$$

$\tau(s)$ is torsion in the Frenet-Serret frame, and $\psi(0)$ is the initial value of torsion and is arbitrary constant of integration. $\kappa(s)$ is curvature, and curvature around the pitch axis $\kappa_p(s)$ and curvature around the yaw axis $\kappa_y(s)$ are expressed as

$$\kappa_p(s) = -\kappa(s)\sin\psi(s),\ \ \kappa_y(s) = \kappa(s)\cos\psi(s). \tag{2}$$

This work was partially supported by Japan Society for the Promotion of Science JSPS KAKENHI [grant number JP21H01285].

K. Yoshida amd M. Tanaka are with the Department of Mechanical and Intelligent Systems Engineering, The University of Electro-Communications, Tokyo, 182-8585, Japan kodai.yoshida@rc.mce.uec.ac.jp, m.tanaka@uec.ac.jp

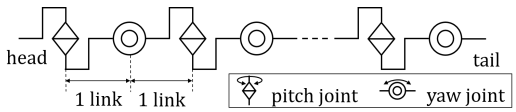

Fig. 1. Structure of the snake robot

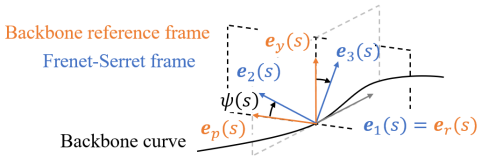

Fig. 2. Difference between Frenet-Serret frame and the backbone reference frame

Therefore, j-th target joint angle θ_j^d is calculated as

$$\theta_j^d = \begin{cases} \int_{s_h+(j-1)l}^{s_h+(j+1)l} \kappa_p(s)\mathrm{d}s & (j:\text{odd}) \\ \int_{s_h+(j-1)l}^{s_h+(j+1)l} \kappa_y(s)\mathrm{d}s & (j:\text{even}), \end{cases} \tag{3}$$

where l is length of each link and s_h is the head position of a snake robot in a continuous curve. By changing s_h, we change the range of approximating the robot to the curve, which is called as *shift motion*. When $\psi(0)$ in (3) is changed, the backbone reference frame rotates around the curve and the robot performs *rolling motion*.

B. Designing a Target Shape Connecting Segments

We design a target shape using the Takemori's method [5] in which simple shapes with known curvature and torsion are connected. Each connected shape is called a *segment*, the j-th segment starting from the robot's tail is defined as "segment-j". $s = s_j$ is the point of *connection part*, which connects segment-$(j-1)$ and segment-j, is expressed as $s_j = s_{j-1} + l_{j-1}$, where l_j is the length of segment-j and $s = s_1$ is the start of segment-1. The curvature and torsion of segment-j are expressed with κ_j and τ_j, and the curvature and torsion of the target shape are expressed as

$$\kappa(s) = \kappa_j,\ \tau(s) = \tau_j \quad (s_j \leqq s < s_{j+1}). \tag{4}$$

The shape of a circular arc is determined by its radius r_j and central angle ϕ_j, and curvature κ_j is $\frac{1}{r_j}$ and torsion τ_j is 0. The shape of a straight line is determined by its length l_j, and curvature κ_j and torsion τ_j are treated as 0.

Next we consider the twist angle at the connection part. $s = s_{j-}$ is the end of segment-$(j-1)$, and $s = s_{j+}$ is the start of segment-j. As shown in Fig. 3, the twist angle between $\boldsymbol{e}_2(s_{j-})$ and $\boldsymbol{e}_2(s_{j+})$ around $\boldsymbol{e}_1(s_{j-})$ is $\hat{\psi}_j$. When considering twisting of segment connection part, $\psi(s)$, which is the twist angle between the Frenet-Serret frame and the backbone reference frame around the $\boldsymbol{e}_1(s)$, is calculated as

$$\psi(s) = \int_0^s \tau(\hat{s})\mathrm{d}\hat{s} + \psi(0) + \sum_j \hat{\psi}_j. \tag{5}$$

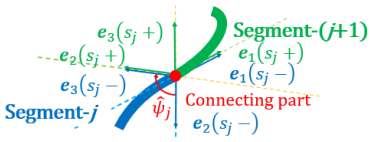

Fig. 3. Torsion of segment connection part

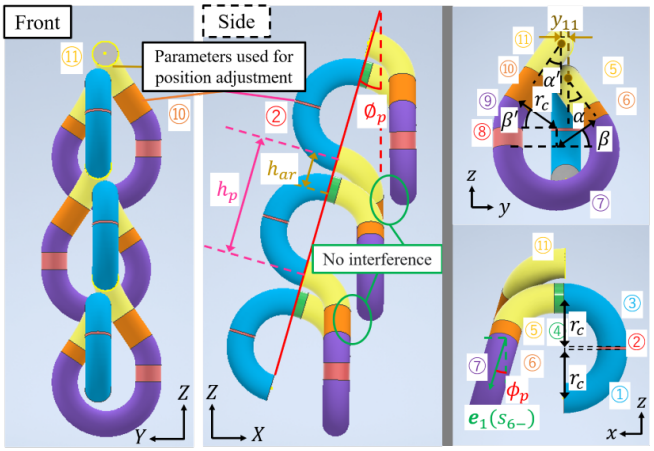

Fig. 4. Target shape for climbing the net

III. Climbing Gait for a Snake Robot

The target shape for climbing a net is shown in Fig. 4. This shape is composed of 11 segments that are repeatedly connected as one unit. Each segment is determined by $r_c, h_p, h_{\text{align}}, l_r, \alpha, y_{11}, \phi_p$, and the parameter is shown in Table I. To prevent the snake robot from falling from a net, the robot's body is passed through the net. After the robot's body enter a mesh, it exits from the same mesh and enters the next mesh.

A. Preventing Cable from Getting Tangled

The snake robot used in this study has a power source cable attached to the robot's tail. The snake robot could not move up the net by winding around the ropes because the cable may become tangled. As proposed in [8], a target shape is designed so that the robot exit from the same mesh to prevent the cable from tangled.

B. Adapting to Deformation of the Entire Net

When the snake robot hangs from the net, the entire net tilts and the mesh deforms in the direction of gravity as shown in Fig. 5. We define the vertical upward direction after the mesh deforms as the Z-axis . We tilt the target shape by ϕ_p, the slope of the reference plane for the target shape, to adapt to the deformation of the entire net. Thus, the snake robot's body does not interfere with itself when the distance to the next mesh is short. In addition, if ϕ_p is large, the snake robots are less likely to get caught on ropes using gravity as shown in Fig. 6 when the head of the robot enters a mesh.

TABLE I

PARAMETERS OF SEGMENTS FOR CLIMBING A NET

type	seg no.j	parameter	$\hat{\psi}_j$
circular arc 1	$11n+1$	$(r_1, \phi_1) = (r_c, \frac{\pi}{2})$	$(-1)^n(\alpha' - \gamma + \pi)$
straight line 2	$11n+2$	$l_2 = h_p - (h_{\text{align}} + 2r_c) + \Delta h$	0
circular arc 3	$11n+3$	$(r_3, \phi_3) = (r_c, \frac{\pi}{2})$	0
straight line 4	$11n+4$	$l_4 = (l_{10} - l_r)\cos\phi_5 + l_8 \sin\phi_p$	0
circular arc 5	$11n+5$	$(r_5, \phi_5) = (r_c, \tan^{-1}(\frac{1}{\cos\alpha \tan\phi_p}))$	$(-1)^n(\alpha - \gamma)$
straight line 6	$11n+6$	$l_6 = l_r$	0
circular arc 7	$11n+7$	$(r_7, \phi_7) = (r_c, \beta + \pi)$	$(-1)^n(\tan^{-1}\left(\frac{1}{\tan\alpha\cos\phi_5}\right) - \pi)$
straight line 8	$11n+8$	$l_8 = \frac{h_{\text{align}} - (l_{10} - l_r)\cos\alpha\sin\phi_5}{\cos\phi_p}$	0
circular arc 9	$11n+9$	$(r_9, \phi_9) = (r_c, \beta')$	0
straight line 10	$11n+10$	$l_{10} = \frac{y_{11}}{\sin\alpha\sin\phi_5} - l_r + 2l_{6s} + \Delta l'$	0
circular arc 11	$11n+11$	$(r_{11}, \phi_{11}) = (r_c, \tan^{-1}(\frac{1}{\tan\phi_p\cos\alpha'}))$	$(-1)^{n+1}(\tan^{-1}\left(\frac{1}{\tan\alpha'\cos\phi_5}\right) - \pi)$

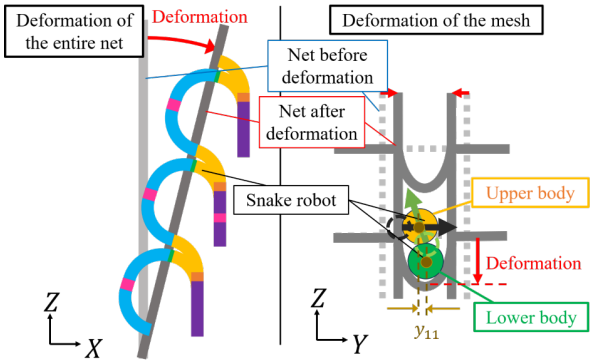

Fig. 5. Deformation of the net

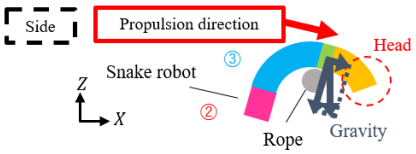

Fig. 6. Entry into the mesh

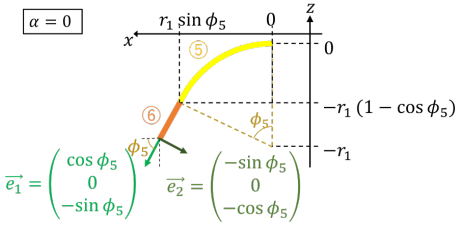

Fig. 7. $\boldsymbol{e}_1(s_{7-})$ when $\alpha = 0$

First, we consider the center angle of circular arc 5 ϕ_5. Fig. 7 shows the tangential unit vector $\boldsymbol{e}_1(s_{7-})$ at the connection part between straight line 6 and circular arc 7. When $\hat{\psi}_5$, the twist angle between straight line 4 and circular arc 5, is rotated α, the unit vector $\boldsymbol{e}_1(s_{7-})$ is calculated as

$$\begin{aligned}\boldsymbol{e}_1(s_{7-}) &= \begin{bmatrix}1 & 0 & 0\\ 0 & \cos\alpha & -\sin\alpha\\ 0 & \sin\alpha & \cos\alpha\end{bmatrix}\begin{bmatrix}\cos\phi_5\\ 0\\ -\sin\phi_5\end{bmatrix}\\ &= \begin{bmatrix}\cos\phi_5\\ \sin\alpha\sin\phi_5\\ -\cos\alpha\sin\phi_5\end{bmatrix}.\end{aligned} \tag{6}$$

The gradient of the z and x components of $\boldsymbol{e}_1(s_{7-})$ is equal to $\tan\phi_p$, thus ϕ_5 is calculated as

$$\phi_5 = \tan^{-1}\left(\frac{1}{\tan\phi_p\cos\alpha}\right). \tag{7}$$

Next, we calculate the twist angle between straight line 6 and circular arc 7 $\hat{\psi}_7$. Since circular arc 7 always exists on a plane where the yz plane is rotated by $-\phi_p$ around the y axis, $\tan\phi_p$ is expressed as

$$\tan\phi_p = -\frac{e_{2x}(s_{7+})}{e_{2z}(s_{7+})}, \tag{8}$$

where the x and z components of $\boldsymbol{e}_2(s_{7+})$ are $e_{2x}(s_{7+})$ and $e_{2z}(s_{7+})$, respectively. Since $\boldsymbol{e}_2(s_{7+})$ is the result of rotating $\boldsymbol{e}_2(s_{7-})$ by $\hat{\psi}_7$ around $\boldsymbol{e}_1(s_{7-})$, $\hat{\psi}_7$ is calculated as

$$\hat{\psi}_7 = \tan^{-1}\left(\frac{1}{\tan\alpha\cos\phi_5}\right). \tag{9}$$

We consider the positional relationship between circular arc 5 and 11 that pass through the mesh. First, we calculate the length of straight line 6 l_{6s} when the positions of circular arc 5 and 11 are overlapped as shown in Fig. 8, where the length of straight line 4 and 10 are 0. Considering that y component of $\boldsymbol{e}_2(s_{7+})$ coincides with $-\cos\beta$, β is expressed as

$$\beta = \cos^{-1}(-\cos\alpha\sin\hat{\psi}_7 - \sin\alpha\cos\phi_5\cos\hat{\psi}_7). \tag{10}$$

The y-coordinate of the connection part of circular arc 6 and 7 coincides with $r_c\cos\beta$, l_{6s} is expressed as

$$l_{6s} = \frac{r_c}{\sin\phi_5}\left\{\frac{\cos\beta}{\sin\alpha} - (1-\cos\phi_5)\right\}. \tag{11}$$

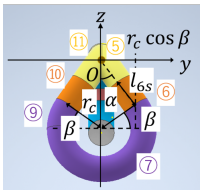

Fig. 8. l_{6s} when the positions of circular arc 5 and 11 are the same

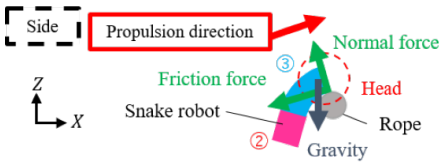

Fig. 9. Failure when a snake robot entries a mesh

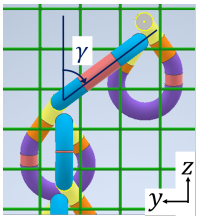

Fig. 10. Angle γ adjustment

Next, we change the position of circular arc 11 by changing the length of straight line 4, 6, 8, 10. The coordinates of circular arc 11 x_{11}, y_{11}, z_{11} relative to circular arc 5 in the part passing through the mesh, are expressed as

$$\begin{aligned} x_{11} &= (l_r - l_{10})\cos\phi_5 - l_8 \sin\phi_p \\ y_{11} &= (l_r + l_{10} - 2l_{6s})\sin\alpha\sin\phi_5 \\ z_{11} &= (l_{10} - l_r)\cos\alpha\sin\phi_5 + l_8\cos\phi_p. \end{aligned} \tag{12}$$

From these formula, l_4, l_8, l_{10} is calculated by considering $h_{\text{align}} = z_{11}$, $l_4 = -x_{11}$. We can change the position of the robot bodies passing through the mesh by altering y_{11} with a condition $|y_{11}| > 0$. As shown in Fig. 5, the y direction of the upper body passing through the mesh is constrained by the left and right ropes and the lower robot body.

C. Adapting to Deformation of the Mesh

As shown in Fig. 5, the mesh deforms in the direction of gravity when the snake robot hangs from the net. To adapt to this deformation, circular arc 5 and 11, which are corresponding to the bodies that pass through the mesh, are arranged in the direction of gravity. As the mesh deforms in the direction of gravity, the distance it takes for the head of the snake robot to enter the next mesh increases. Therefore, Δh, which is initially set to 0, is increased as necessary.

D. Adjusting the Head Position of the Snake Robot

When the head of the snake robot enters the mesh, we increase Δh to compensate the position error influenced by the gravity and reduce contact with ropes. If the head of the snake robot contact the ropes while facing diagonally upwards as shown in Fig. 9, the propulsion force is reduced and the head of the snake robot could not enter the mesh due to the friction and normal force. After the robot enters the mesh, we restore Δh.

When the snake robot exits from the mesh, we increase the center angle of circular arc 9 β' and $\Delta l'$ to move the head in the y direction towards the center of the mesh. $\Delta l'$ is initially set to 0. After the robot exits from the mesh, we restore these parameters.

In this way, the operator adjusts $\Delta h, \beta', \Delta l'$, but when exposed to external vibrations such as wind, the adjustments by the operator become more difficult.

E. Selecting the direction of movement

When the snake robot move on the net, it is required to move not only vertically but also horizontally. By adjusting γ as shown in Fig. 10, the head of the snake robot can move to an arbitrary direction of mesh. When the snake robot move vertically, γ is set to 0.

IV. Experiment

We performed experiments by using the snake robot shown in Fig. 11 to verify the proposed net climbing gait. This was developed by Takanashi et al. [6] and uses the structure devised by Takemori et al. [8].

A. Vertical Movement

Experiments of the snake robot climbing vertically on the net with the mesh's vertical and horizontal lengths of 100 mm, 135 mm and 200 mm. The parameters were $r_c = 90$ mm, $h_{\text{align}} = 65$ mm, $l_r = 30$ mm, $\alpha = 35°$, $y_{11} = -15$ mm. h_p was set according to the size of the mesh. ϕ_p was set to $\phi_p = 16°$ so that the snake robot bodies don't interfere with each other, but the value was changed in some experiments.

First, the experimental result using the net with its mesh's vertical and horizontal lengths of 100 mm are shown in Fig. 12. The snake robot successfully performed a series of operations from entering the mesh to exiting the mesh. By tilting the target shape by ϕ_p, the head of the snake robot did not fall in the x and y directions before entering the mesh. Also, by tilting the target shape, the snake robot was able to enter the mesh smoothly with the help of gravity as shown in Fig. 6. The head of the snake robot entered the mesh by increasing the length of Δh and without adjusting γ at $t = 60$ s. Also, the head of the snake robot exited from the mesh by increasing the center angle of circular arc 9 and the length of straight line 10 at $t = 170$ s. On the other hand, some problem arose. The head of the snake robot stuck when the head contact the rope above it at $t = 10$ s. This is thought that the propulsion force could not be obtained for the head to enter the mesh if the robot's head contact with the ropes as shown in Fig. 9. However, the problem was resolved by a rolling motion. Besides, the part near the head of the snake robot frequently got caught in the ropes after $t = 70$ s. In

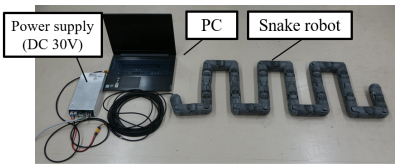

Fig. 11. Snake Robot

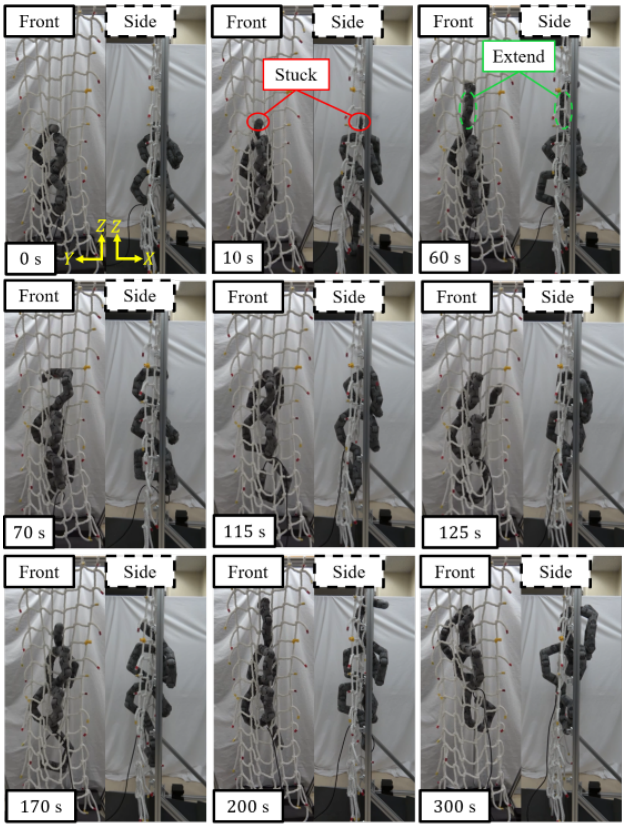

Fig. 12. Vertical movement(Mesh 100mm)

addition, the head fell in the negative direction of the Y axis from $t = 100$ s to $t = 125$ s. The current and joint angles at this time are shown in Fig. 13 and Fig. 14. From $t = 100$ s to $t = 125$ s, the current became considerably large mainly at the 7-th joint and could not follow the target value. It is thought that the torque of the motor being used is insufficient.

To consider differences in movement due to differences in body shape inclination, we performed experiments with $\phi_p = 20°$ and $\phi_p = 24°$ in addition to $\phi_p = 16°$. As shown in Fig. 15, in the experiments when $\phi_p = 20°$ and $\phi_p = 24°$, the robot failed to exit from the mesh. This is thought to be because the inclination of the target shape ϕ_p was too large for the deformation of the net. Therefore, it is considered better to make ϕ_p as close to the deformation of the net as possible.

Next, the experimental result using the net with its mesh's vertical and horizontal lengths of 135 mm are shown in Fig. 16. We performed the same action as in the experiment

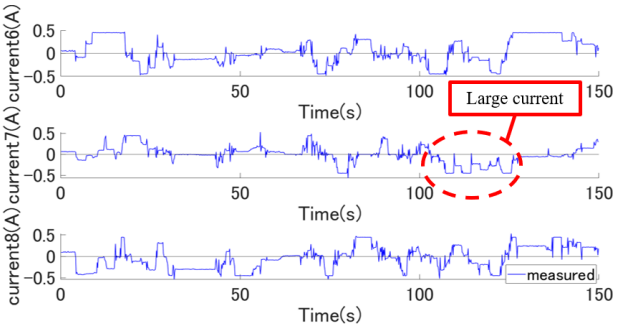

Fig. 13. Joint 6-8 current

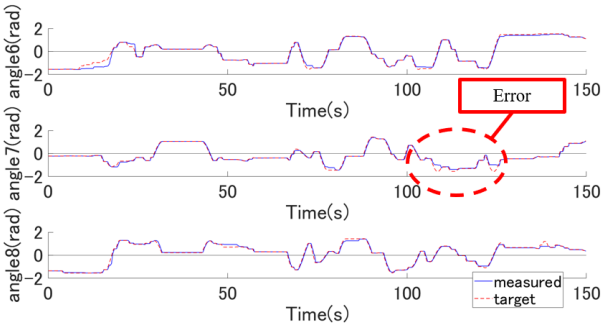

Fig. 14. Joint 6-8 angle

using the net with its mesh's vertical and horizontal lengths of 100 mm, and succeeded in a series of operations from entering the mesh to escaping. On the other hand, some problems occurred that did not occur with the 100 mm mesh. The robot got caught on the rope in the area circled in red in Fig. 16 at $t = 20$ s, and the head of the snake robot fell in the negative direction of the X axis. It is thought that the larger the mesh size, the larger the contact area between the rope and the robot which causes the robot gets caught.

Finally, the experimental result using the net with its mesh's vertical and horizontal lengths of 200 mm are shown in Fig. 17. At the start of shift motion, the head of the snake robot moved away from the net, and even after adjusting the position, it was not possible to exit from the net. The robot's body is heavier on the back side of the mesh than on the front side, so it is thought that the head of the robot fell toward the back side. In experiments when the length of the mesh is 100 mm or 135 mm, the robot's body touches the top part of the mesh while exiting. However, in experiments when the length of the mesh is 200 mm, the robot's body did not touch the top part of the mesh and fell in the direction of the X axis.

B. Movement in diagonal Direction

We performed a experiment that snake robot moved in diagonal direction using the net with its mesh's vertical and horizontal lengths of 100 mm. The parameters are the same as in the vertical movement experiment. By changing γ, it was possible to enter any mesh as shown in Fig. 18.

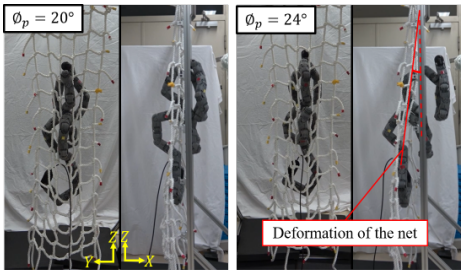

Fig. 15. Failure to exit from the mesh($\phi_p = 20°, 24°$)

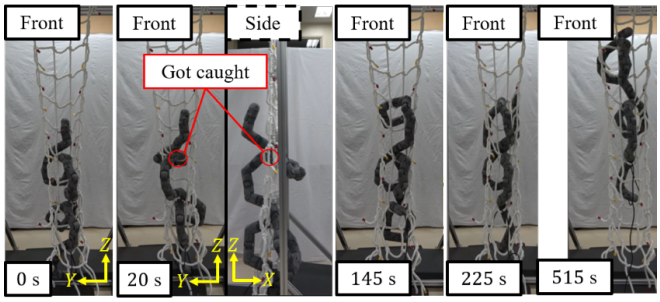

Fig. 16. Vertical movement (Mesh 135mm)

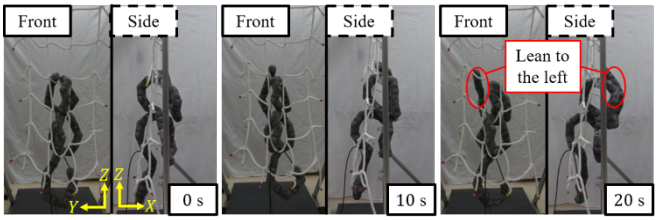

Fig. 17. Vertical movement (Mesh 200mm)

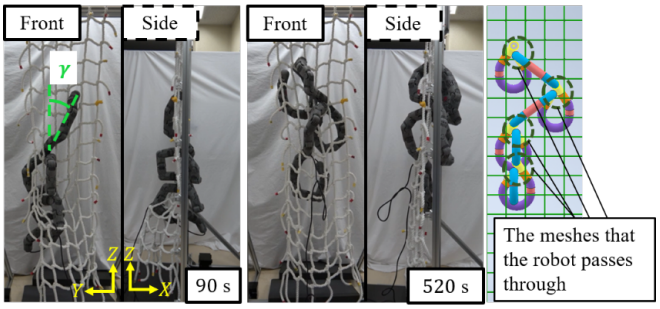

Fig. 18. Movement in diagonal direction

V. Conclusions

We proposed a climbing gait for a snake robot to adapt and move on a flexible net. The proposed gait prevents the cables from tangled with the net. The robot can also adapt to the deformation of the entire net and mesh by changing adjusting the parameters. We performed experiments to demonstrate the effectiveness of the proposed method, and showed that a snake robot could move not only vertically but also in diagonal direction on a net.

One of the future works will be to experiment with ropes made of different materials. Also, the control of a snake robot during experiments is complicated, simplifying the operation will be our future work. Another challenge for the future is to attach cameras and other devices to the robot to enable remote control. However, there is a problem that the joint angle cannot follow the target value due to insufficient torque, and the success rate of moving the net decreases. We will also work on simplifying the control for remote control.

References

[1] H. Kajiwara, M. Arai, T. Noguchi, and T. Nakamura, "Development of Rockfall Prevention Net Climbing Robot Using a Quadric Chain," *J. of Robotics and Mechatronics*, vol. 18, no. 3, pp. 312–317, 2006.

[2] N. Kaya, M. Iwashita, S. Nakasuka, L. Summerer, and J. Mankins, "Crawling Robots on Large Web in Rocket Experiment on Furoshiki Development," in *Proc. Int. Astronautical Congress*, 2004, pp. 402-406.

[3] Q. Fu, Y. Guan, and H, Zhu, "A Novel Robot with Rolling and Climbing Modes for Power Transmission Line Inspection," in *Proc. IEEE/RSJ Int. Conf. on Intelligent Robots and Systems*, 2022, pp. 7122–7128.

[4] S. Farzan, V. Azimi, A. Hu, and J. Rogers, "Adaptive Control of Wire-Borne Underactuated Brachiating Robots Using Control Lyapunov and Barrier Functions", *IEEE Trans. on control systems technology*, vol. 30, no. 6, pp. 2598–2614, 2022.

[5] T. Takemori, M. Tanaka, and F. Matsuno, "Gait Design for a Snake Robot by Connecting Curve Segments and Experimental Demonstration", *IEEE Trans. on Robotics*, vol. 34, no. 5, pp. 1384–1391, 2018.

[6] T. Takanashi, M. Nakajima, T. Takemori, and M. Tanaka, "Obstacle-Aided Locomotion of a Snake Robot Using Piecewise Helixes," *IEEE Robotics and Automation Letters*, vol. 7, no. 4, pp. 44150–44166, 2018.

[7] J. Løwer, I. Gravdahl, D. Varagnolo, and Ø. Stavdahl, "Form Closure for Fully Actuated and Robust Obstacle-Aided Locomotion in Snake Robots," *IEEE Robotics and Automation Letters*, vol. 8, no. 11, pp. 7360–7367, 2023.

[8] T. Takemori, M. Tanaka, and F. Matsuno, "Ladder Climbing with a Snake Robot", in *Proc. IEEE/RSJ Int. Conf. on Intelligent Robots and Systems*, 2018, pp. 8140–8145.

[9] Y. Wang, T. Kamegawa, E. Matsuda, and A. Gofuku, "Motion planning of a snake robot that moves in crowded pipes," *Advanced Robotics*, vol. 36, no. 16, pp. 781–793, 2022.

[10] M. Inazawa, T. Takemori, M. Tanaka, and F. Matsuno, "Unified Approach to the Motion Design for a Snake Robot Negotiating Complicated Pipe Structures," *Frontiers in Robotcs and AI*, vol. 8, pp. 1–18, 2022.

[11] S. Zou, W. Xi, X, Guo, and Y. Fang, "Manipulation Using a Snake Robot Based on the Head Raising Motion," in *Proc. Asia-Pacific Conf. on Intelligent Robot Systems*, 2022, pp. 170–175.

[12] T. Takemori, M. Tanaka, and F. Matsuno, "Hoop-Passing Motion for a Snake Robot to Realize Motion Transition Across Different Environments," *IEEE Trans. on Robotics*, vol. 347, no. 5, pp. 1696–1711, 2021.

[13] B. A. Elsayed, T. Takemori, and F. Matsuno, "Gait Recovery for a Snake Robot With Multiple Failed Joints," *IEEE/ASME Trans.on Mechatronics*, pp. 1–12, 2023, [Online early access].

[14] T. Abe and H. Date, "Visualization system in a third-person view for the teleoperation of a snake-like robot," *Advanced Robotics*, vol. 36, no. 16, pp. 751–766, 2022.

[15] R. Watanabe and M. Tanaka, "Principle of object support by Rope deformation and its application to Rope climbing by snake robot," *Advanced Robotics*, vol. 37, no. 9, pp. 591–602, 2023.

[16] H. Yamada and S. Hirose, "Study of Active Cord Mechanism — Approximations to Continuous Curves of a Multi-joint Body, "*J. of the Robotics Society of Japan*, vol.26, no.1, pp.110–120, 2008. (in Japanese with English Summary)